Characteristisation of a recirculating flow using ultrasonic Doppler velocimetry

Xiaodong Wang, Yves Fautrelle & Jacqueline Etay

EPM/SIMAP/CNRS/INPG/ENSEEG laboratory,
B75, 38402 Saint Martin d'Hères cedex, France

Corresponding author: Xiaodong Wang, E-mail: xiaodong.wang@hmg.inpg.fr

Abstract:
We deal with a metallic GaInSn flow driven by a traveling magnetic field. The flow field in a parallelipedic box was measured by ultrasonic Doppler velocimetry. The mean velocity profiles and fluctuating behavior are obtained. The mean velocity is influenced by the pole pitch of the linear motor. The magnetic field distribution is measured and the Lorentz force is analyzed. The turbulent character of the flow is confirmed by discrete Fourier analysis of the registered signal, the flow exhibits continuous frequency spectrum.

Résume:
Nous traitons un écoulement métallique de GaInSn dans une boîte parallelipedic mise en mouvement par un champ magnétique glissant. Le champ de vitesse a été mesuré par vélocimétrie Doppler ultrasonique. Les profils de vitesse moyenne et le comportement de fluctuation sont obtenus. La vitesse moyenne est influencée par le pas polaire du moteur linéaire. La distribution de champ magnétique est mesurée et la force de Lorentz résultante est calculée. Le caractère turbulent de l'écoulement est confirmé par l'analyse de Fourier discrète du signal enregistré. L'écoulement se présente un spectre fréquence continu.

Key-words:
traveling magnetic field; liquid metal; Ultrasonic Doppler velocimetry

Mot-clés:
champ magnétique glissant; métal liquide ; Doppler Ultrasonique Velocimetry

1   Introduction

The application of electromagnetically driven convection on liquid metal, the so-called electromagnetic stirring, has been widely used in metallurgy. Electromagnetic stirring may be generated by two kinds of devices, namely the single–phase or polyphase inductors. Concerning polyphase inductors, they can generate either traveling or rotating magnetic fields. Electromagnetic stirring is used for example in ladle metallurgy for liquid metal refining to promote transfer reactions through the interface between a liquid metal and a covering slag or molten salt (Fautrelle Y., Perrier D. & Etay J. 2003). A widespread application also concerns the continuous casting of steel where electromagnetic stirring, rotating or traveling magnetic fields were used either near the mold or in the mid-part of the liquid sump. One of the general goals of the application of stirring is to act on the solidification of the liquid metal.

We present hereafter measurements of the flow field in a rectangular liquid metal pool submitted to a linear motor. We are interested in the turbulent flow driven by the traveling magnetic field.

Flow measurements are carried out by using of UDV-Ultrasonic Doppler Velocimetry (DOP2000), which is a very efficient tool to measure velocity in opaque fluid such liquid metals as mercury (Takeda Y. 1987), gallium (Brito D. & Nataf H.C. 2001) or sodium (Eckert S. & Gerbeth G. 2002). We will introduce the experiment configuration, the description of the velocimetry method, and then the characteristics of flow are analyzed.

2   Experimental set-up and measurement procedure

2.1 Experimental set-up

The experimental set-up is presented on FIG.1. A liquid metal of 67*wt.*%Ga-20.5*wt.*%Sn-12.5*wt.*%In is contained in a transparent rectangular cavity of *W*=1*cm* in width, *L*=10*cm* in length, and *H*=6*cm* in height. The origin of the coordinates is located at the left-bottom corner within the meridian plane. The physical properties of the alloy are given in table 1.

The Linear Induction Motor (LIM) used to generate a traveling magnetic field is a three-phase linear motor (LMS13, HIWIN[®]), which is installed at 5*mm* under the bottom of the cavity. The nominal electric current used in the stirrer is *I* =3, 4, 5*A* (r.m.s. value) at a frequency of 50*Hz*. $\left\|\vec{B}\right\| = \sqrt{B_x^2 + B_y^2}$ in different z positions have been measured in the absence of metallic alloy as illustrated in FIG.2. The magnetic field distribution closed to the bottom of the liquid bulk is strongly affected by the magnetic poles positions, as z increases, the influence becomes weak. The horizontal position of the liquid bulk also noted in FIG.2.
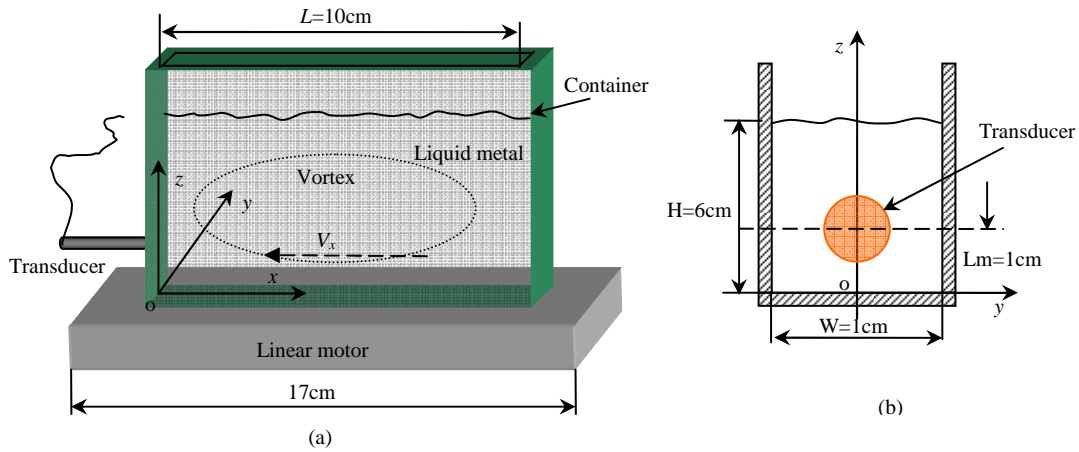

FIG.1 – Schematic view of the experimental arrangement

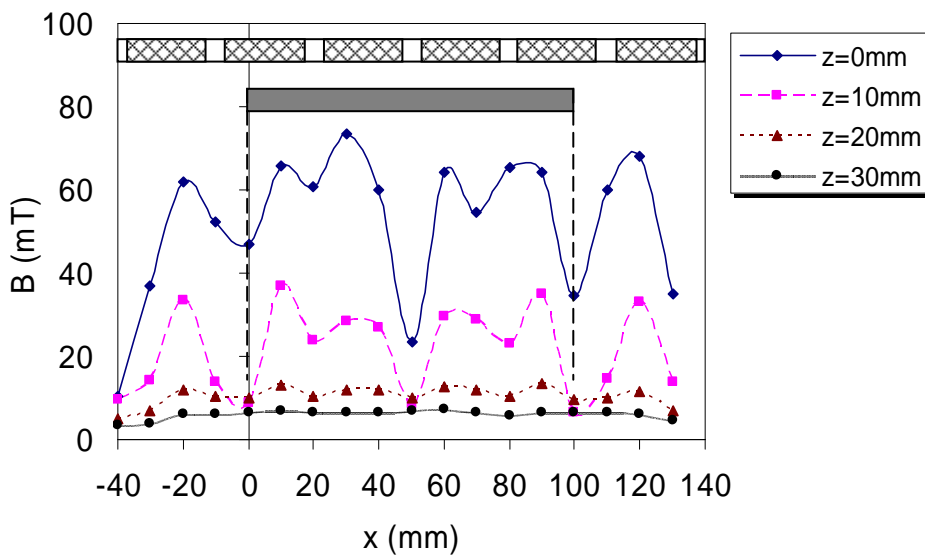(a)   Front view; (b) transverse view

FIG.2 – Measured distribution of the magnetic field amplitude $\left\| \vec{B} \right\|$ in the z-direction, the inductor with six magnetic poles and the location of the liquid bulk are illustrated. *I*=4A (r.m.s. values).

Table1. - Physical properties of GaInSn alloy

Properties and symbols	Values and Units
Melting point, T_m	10.5 °C
Density, ρ	$6.4 \times 10^3 \, kg/m^3$
Electrical conductivity, σ	$3.4 \times 10^6 \, (\Omega \cdot m)^{-1}$
Kinematic viscosity, υ	$3.4 \times 10^{-7} \, m^2/s$
Sound speed, c	2860 *m/s*
Surface tension, γ	$0.533 \, N \cdot m^{-1}$

2.2 Description of the velocimetry method

The ultrasonic transducer is placed in one of the sidewalls in the horizontal direction, which is a 4-*MHz* probe, 8*mm* in diameter. According to relationship between wavelength and frequency $\lambda f = c$, c being the sound speed in the liquid metal, we deduce that the wavelength is 0.715*mm*. Then, the spatial physical resolution in the shooting direction reaches 2×0.715 = 1.43*mm* in the liquid metal, each profile consists of 64 points, thus the total length of investigation is $1.43 \times 64 = 91.52mm$, therefore a measuring blind zone exists near the wall in the presence of the transducer. We adjust the parameters of Doppler apparatus, namely the pulse repetition frequency (PRF), the cycles, the profiles, and the emissions per profiles to obtain optimal velocity signal. PRF is an essential parameter, the time t_{PRF} between two emissions not only determines the length of the profile, but also controls the velocity resolution (Brito D. & Nataf H.C. 2001). Only the velocity component parallel to the ultrasonic beam is accessible in present study. The velocity component in the *x*-direction V_x is measured and analyzed. Note that small heterogeneities (i.e. oxide particles) in the bulk liquid are necessary in order to obtain significant echoes.

Table 2. lists the main control parameters. The V_x velocity component is measured along a horizontal line (*y* = 0, *z* = 10*mm*). On the other hand, we have observed that the fringe effect exists near the left vertical wall in which ultrasonic transducer is installed. It causes a perturbation near the wall but does not affect significantly the measured velocity value in the centre part.

Table 2. - Ultrasonic Doppler velocimetry parameters for liquid metal GaInSn

Physical properties	values
Wavelength	0.715 *mm*
Pulse cycles	2
t_{PRF}	728 *μs*
points per profile	64
Total measurement time	64.7*s*

We can estimate the turbulence kinetic energy from the root-mean-square velocity Then if we assume that the turbulence kinetic energy distribution k is isotropic in space (the latter assumption may strongly overestimate k), its order of magnitude is given by

$$k \approx \frac{3}{2} \tilde{V}_x^2 \qquad\qquad\qquad (1)$$

Fast Fourier Transform is used to analyze the frequency content of the signals. Fourier spectrum indicates the fluid flow characters (turbulence or not). Since we obtain the velocities values in discrete data, the velocity value are adopted among each interval time $\Delta t = 64.7ms$, the DFT (Discrete Fourier Transform) method was adapted by mean of software MATLAB7.0©.

3 The flow analysis

3.1 Lorentz force generated by a single linear inductor

Firstly, let us estimate the electromagnetic force amplitude in the present study. To that purpose, we consider the similar case of an ideal linear stirrer (Dubke M. & Tacke K.H. 1988). In case of the inductor being considered as infinitely long and neglecting the back influence of the motion on the current density, the *x*-component of the electromagnetic force density is such that:

$$F_x = F_0 e^{-2\alpha z}\left(1 + \cos\left(2\omega t - 2\lambda x\right)\right) \ \text{With } F_0 = \frac{\sigma\omega}{2\lambda}B_0^2, \ \alpha = \Re e\left(\sqrt{i\mu\sigma\omega + \lambda^2}\right) \qquad (2)$$

In our case, the liquid metal flow is limited in a narrow domain, which increase α so much, therefore F_x decrease significantly than the case in infinite liquid bulk width; λ is the wavelength of the magnetic field, due to $2\tau = 32mm$, thus $\lambda = 2\pi / 2\tau = 196m^{-1}$, μ magnetic permeability, σ electric conductivity, $\omega = 2\pi f_e$, f_e magnetic frequency, B_0 applied magnetic field strength, *i* unit of complex number $i^2 = 1$. The ratio $\dfrac{\mu\sigma\omega}{\lambda^2} = 0.017$ is much less than unit, therefore the value of the skin depth δ is imposed mainly by the pole pitch rather than by the frequency. The skin depth is

$$\delta = \frac{1}{\alpha} \approx \frac{1}{\lambda} = 5.1mm \qquad (3)$$

When the current *I* is equal to 4.0*A* for example, then we have $B_0 = 25$ *mT* (cf. FIG.2), $f_e = 50Hz$, and thus the order of the corresponding amplitude of the electromagnetical force is about: $F_x \sim O(10^2 \sim 10^3)N/m^3$.

3.2 Mean flow behavior

FIG.3(a) illustrated the time evolution of the instantaneous velocity for *I* = 4*A* at P(0.05, 0, 0.1), The instantaneous velocities vary in a large range from -18 to -35 mm/s, the mean velocity $\overline{V}_x$ is -26.4 *mm/s*. On FIG.3(b), $\overline{V}_x$ profile one are plotted for three values of the inducting electrical current I = 3, 4 and 5A. These three profiles are similar in shape, when intensity magnitude increases as *I* increase.

From the shape of the profile we may say that the mean flow exhibits a large central vortex associated to two smaller and weaker vortices located near the bottom corners. It is not clear if the vortices are driven by viscosity or are generated by electromagnetic force gradient associated to the geometry of the polar pitch of the inductor.
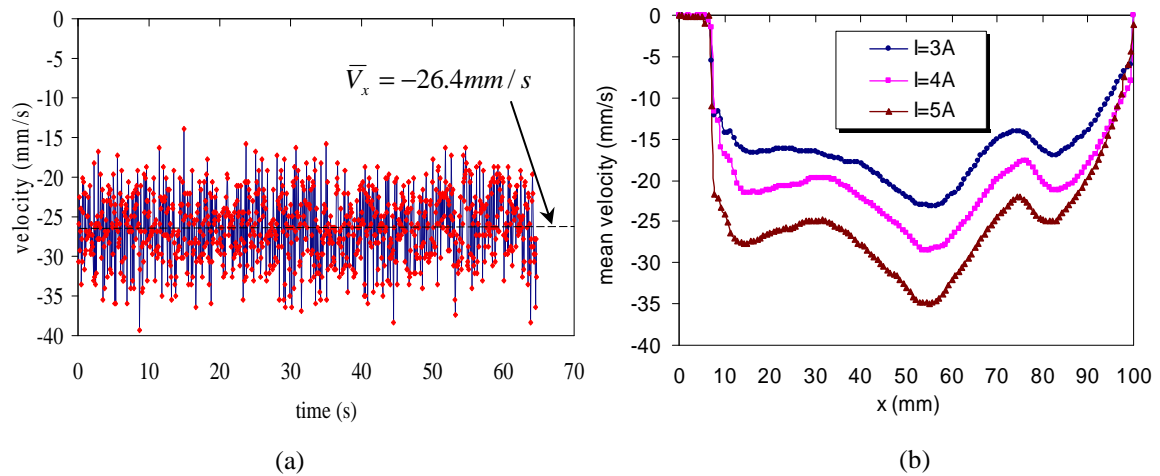
(a)   (b)

FIG.3 - Velocity behaviors: (a) instantaneous velocity at P(0.05, 0, 0.1) $I = 4A$; (b) longitudinal mean velocity profiles for various magnetic field intensities.

3.3 Turbulence characteristics

We plotted dimensionless quantity $\tilde{V}_x / \overline{V}_x$ as illustrated in FIG.4(a), the collected profiles explicit that the fluctuation intensity is proportional to the mean $\overline{V}_x$, and they have $\tilde{V}_x \approx 10\% \overline{V}_x$. Duo to fringe effect, the fluctuation near the right sidewall seems stronger, but we have not observed the ideal symmetrical situation on the left side, it may cause the registered signal of UDV.

The turbulence kinetic energy k computed according to Equ.(1~3). DFT analysis indicates that the energy spectrum of V_x is continuous as illustrated in FIG.4(b), which confirms that the flow is turbulent. This point can also be proved by high value of Reynolds number in the present case:

$$\mathrm{Re}_x = \frac{\overline{V}_x H}{\nu} = 4590 \qquad\qquad (4)$$

Where the typical order of the *x*-component velocity $\overline{V}_x$ is chosen as 25 *mm/s*.

Regarding to the theoretical model of Kolmogorov spectrum for sufficiently developed turbulence flow, as in Ref.(Felten F. & Fautrelle Y. 2004), the curve of the typical frequency energy spectrum $E(f)$ yields a short plateau, and decays with a slope (-5/3) as the function of the bulk liquid frequency in inertial zone. In a like-manner, here, a mono-directional spectrum of the velocity fluctuation is calculated with 15 experiment series (namely 15 events). As illustrated in figure6, $E(f)$ curve of the present calculating result. There exist a sharply decays with approximately exponent slope (-1.9). The value of this slope is a little bigger than that (-5/3) in the Ref.[19], that may cause of mono-spectrum, the turbulence did not fully developed in other direction. After that, it reaches to the viscosity zone; we observed an energy peak near one hertz, which is corresponding to the flow turnover time. The order of flow turnover time in the cavity can be estimated by the ratio between the typical length of the box and the typical velocity of the flow:

$$\tau = O\left(\frac{L}{\overline{\overline{V}}_x}\right) \tag{5}$$

The energy peak shows this turnover time is about 1.2 *s*.
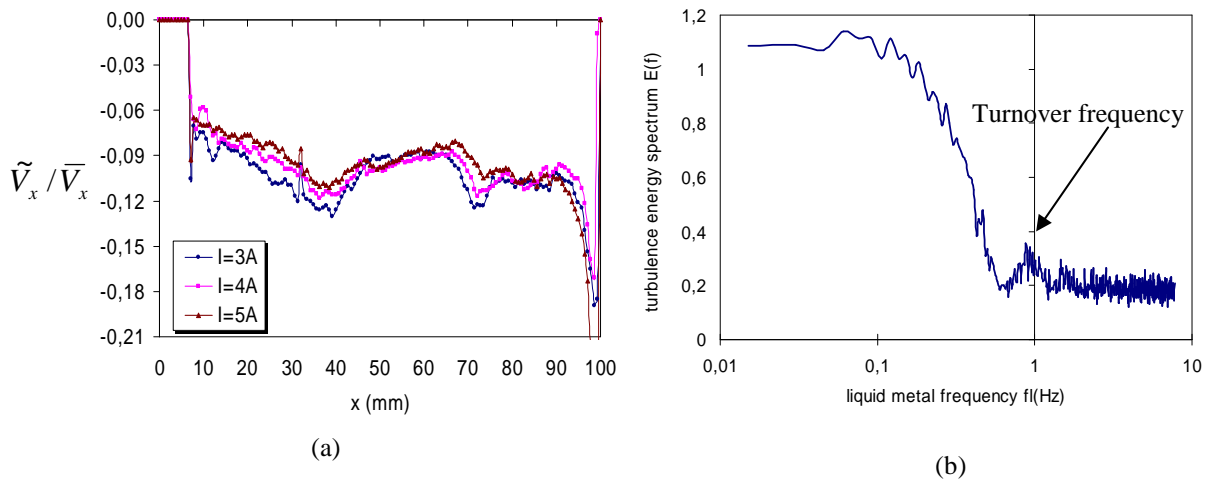

(a)

(b)

FIG.4-Turbulent flow behaviors: (a) dimensionless quantity $\widetilde{V}_x / \overline{V}_x$ comparison for various electromagnetical intensities; (b) mono-directional spectrum of the velocity fluctuation.

4. Conclusion

The flow of the metallic liquid GaInSn alloy submitted to a traveling magnetic field was studied. The *x*-component velocities measured by mean of UDV, and its mean values and fluctuations are analyzed. The magnetic force is calculated base on the electromagnetic parameters, and its order is estimated. Analysis of Discrete Fourier transform indicated the energy spectrum of this type flow yields turbulent characteristics. Such flow is used to control solidification for instance by [Zaidat K and Moreau R].

References:

Brito D., Nataf H.C. 2001 Ultrasonic Doppler velocimetry in liquid gallium. *Experiments in Fluids*. **31,** 653-663

Dubke M., Tacke K.H and Schwerdtfeger K. 1988 Flow field in electro, magnetic stirring of rectangular strands with linear inductors: part 1. Theory and experiments with cold models. *Met. Trans. B* **19B,** 581- 593

Eckert S. Gerbeth G. 2002 Velocity measurements in liquid sodium by mean of ultrasonic Doppler velocimetry. *Experiment in Fluids*. **Vol.32 No.5**, 542-546

Fautrelle Y., Perrier D. & Etay J. 2003 Free surface controlled by magnetic fields. *ISIJ international.* **Vol.43 No.6**, 801-806

Felten F., Fautrelle Y. 2004 Numerical modelling of electromagnetically-driven turbulent flows using LES methods. *Applied mathematical modelling*. **28,** 15-27

Takeda Y. 1987 Development of velocity profile of mercury flow by ultrasonic Doppler shift method. *Nuclear Technique*. **79,** 120-284

Zaidat K. 2005 The influence of the travelling magnetic field on the directional solidification of the binary alloy. *Ph.D. thesis, EPM, France*, 43-67